Where are the proto-South China Sea slabs? SE Asia plate tectonic and mantle flow history from global mantle convection numerical modeling

Yi-An Lin[1] (ylin51@uh.edu), Lorenzo Colli[1], Jonny Wu[1]
[1]University of Houston, Department of Earth and Atmospheric Sciences

UNIVERSITY of HOUSTON EARTH and ATMOSPHERIC SCIENCES

Paradigm

Grant 1848327

Summary

• The plate tectonic history of the hypothesized 'proto-South China Sea' (PSCS) ocean basin and surrounding SE Asia since Cenozoic times is controversial.
• We implement four diverse PSCS plate reconstructions into global geodynamic models to constrain PSCS plate tectonics and possible slab locations.
• The double-sided PSCS subduction models with late Oligocene initiation of Borneo counterclockwise rotations and smaller reconstructed Philippine Sea plate sizes can better reproduce the SE Asian mantle structure.
• Double-sided PSCS subduction combined with earlier Borneo rotations uniquely reproduces sub-horizontal slabs under the southern South China Sea at ~400 to 700 km depths; these models best fit seismic tomography.
• A smaller Philippine Sea (PS) plate 37 with a ~1000 km-long restored Ryukyu slab was superior to a very large PS plate.

1. Introduction

1.1 Regional Tectonic Settings

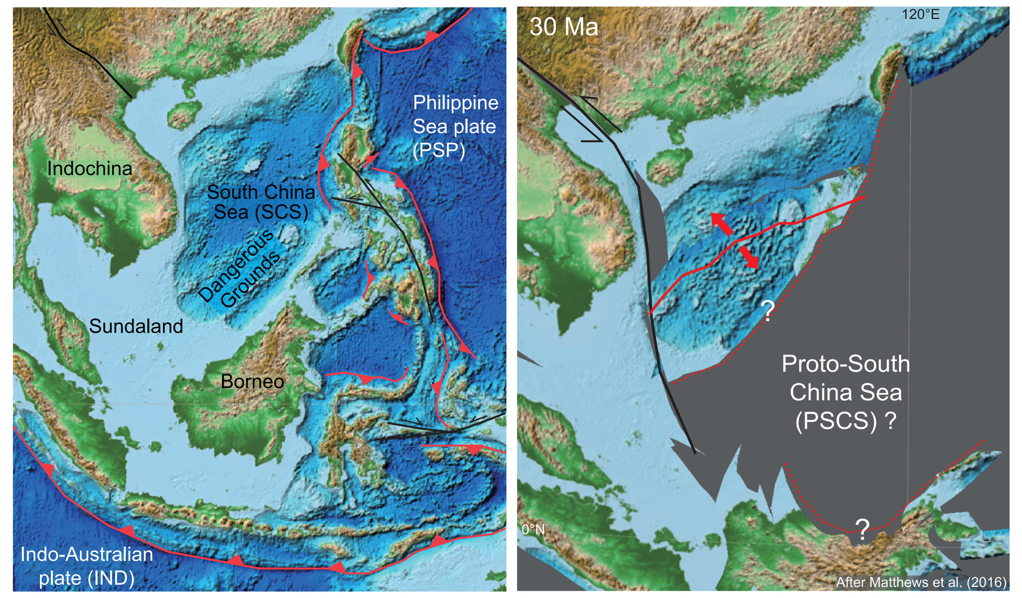

• Reconstructions back to 30 Ma imply the possible existence of a proto-South China Sea.

1.2 Proposed proto-South China Sea plate model ?

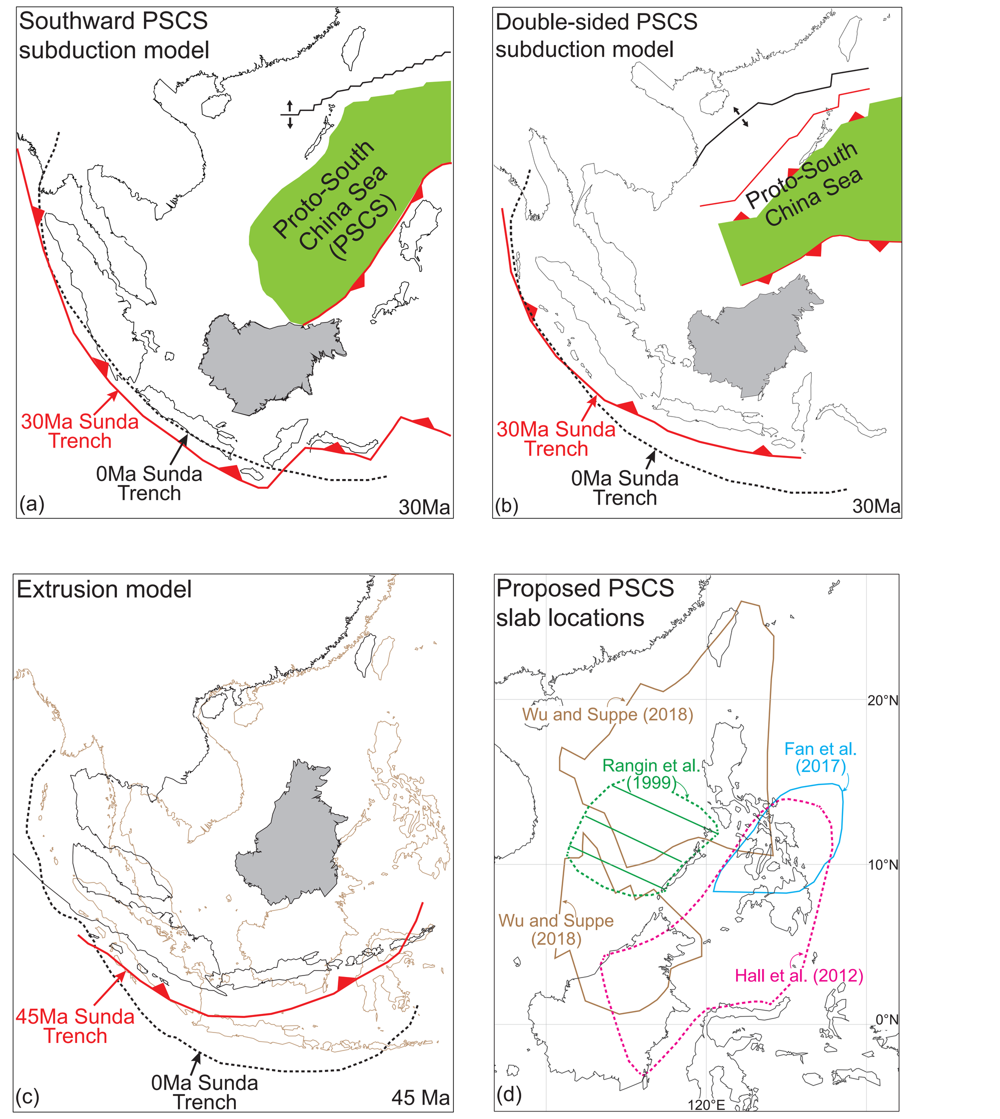

• (a) Southward subduction model; (b) Double-sided subduction model; (c) Extrusion model; (d) Previous interpretation of the seismic tomography model for the PSCS slab in the mantle suggested it to be at ~500 km depth beneath present-day SCS by Rangin et al. (1999); at ~800 km depth central Borneo trending SW-NE to central Philippines based on UUP07 P-wave tomography model by Hall and Spakman (2015); at 400-700 km depth beneath Luzon islands based on regional P-wave tomography model by Fan et al. (2017); proto-South China Sea north slab (N-PSCS) at ~500 km depth beneath present-day SCS and proto-South China Sea south slab (S-PSCS) at ~800 km depth beneath southern SCS based on MITP08 P-wave tomography by Wu and Suppe (2018). Solid lines are the PSCS slabs of previous interpretation and the dashed lines are the inferred sizes.

1.3 Aims and Approach

• In this study we explored the contrasted plate tectonic reconstructions proposed for the proto-South China Sea and Southeast Asia.
• Four different end-member plate models were implemented into global geodynamic models to test their predicted mantle structure against seismic tomography.

1.4 Contrasted Plate Models in SE Asia

Possible proto-South China Sea subduction configuration

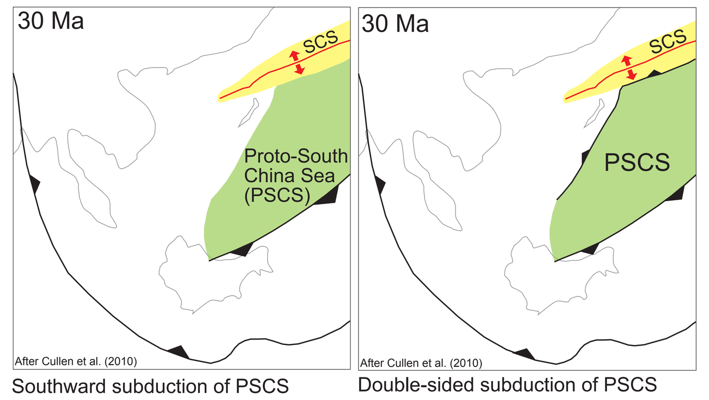

Southward subduction of PSCS — Double-sided subduction of PSCS

Proposed Borneo rotation style

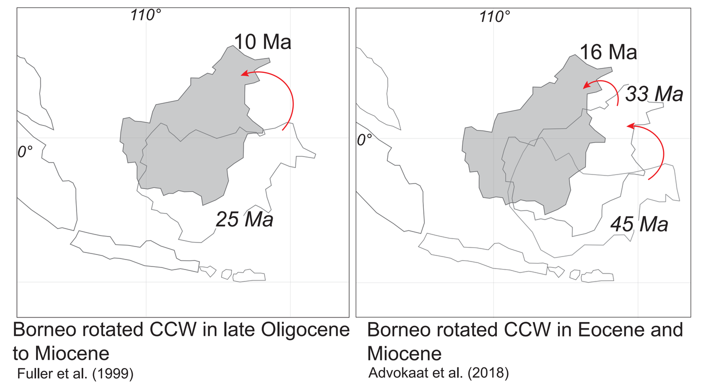

Borneo rotated CCW in late Oligocene to Miocene (Fuller et al. (1999)) — Borneo rotated CCW in Eocene and Miocene (Advokaat et al. (2018))

End-member Philippine Sea plate sizes

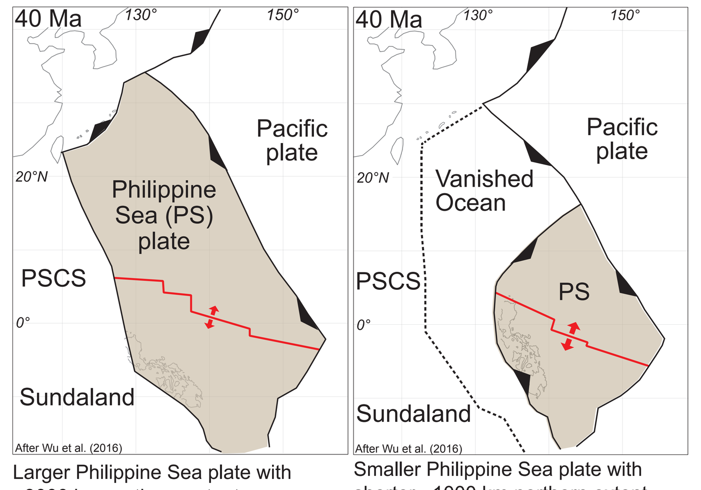

Larger Philippine Sea plate with >3000 km northern extent — Smaller Philippine Sea plate with shorter ~1000 km northern extent

• Southeast Asian plate tectonic reconstruction parameters implemented into the geodynamic models in this study. (a) and (b) show the southward PSCS subduction and double-sided PSCS subduction models, respectively; (c) and (d) show later and earlier proposed Borneo counterclockwise rotations, respectively; and (e) and (f) show proposed larger and smaller end-member Philippine Sea (PS) plate sizes, respectively.

2. Methods

2.1 Numerical Mantle Flow Model

• Input: Global plate model
Fixed slip surface
Not imposing dip angle for the trench
Calculating the conservation of mass, energy and momentum using TERRA
• Output: 4D global mantle thermal structure and flow field

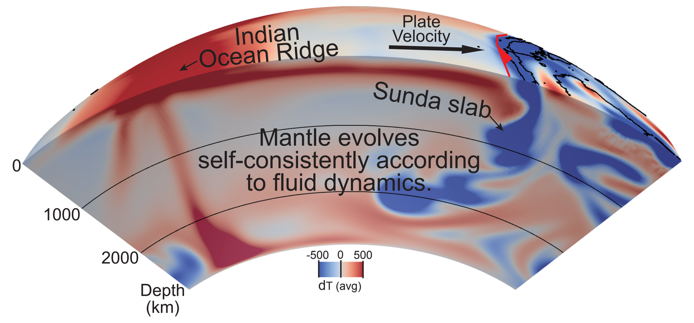

2.2 Dynamic Topography

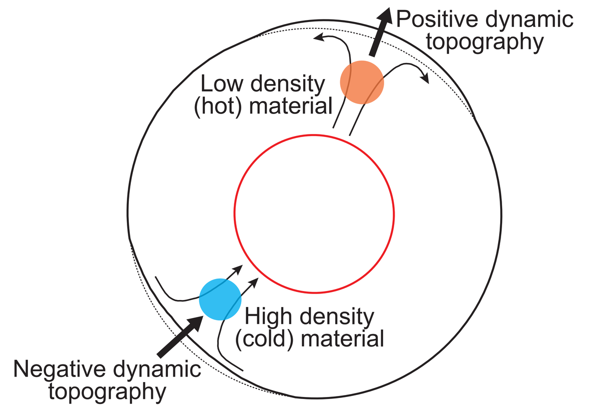

2.3 Input Kinematic Boundary Condition

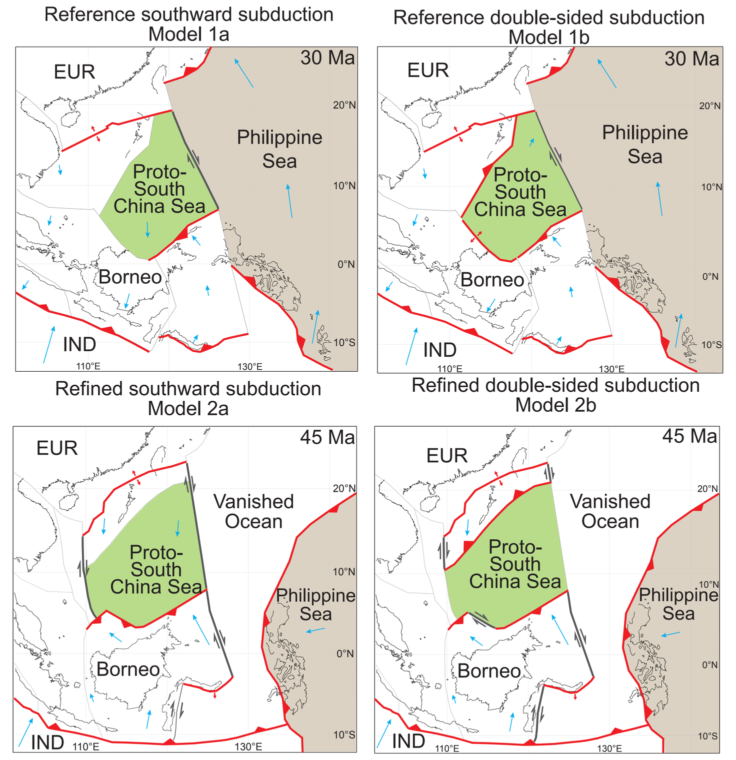

2.4 List of Kinematic Models

Model Name	Borneo CCW Rotation	PSCS Subduction	Philippine Sea Plate Size	Initial State
Reference Southward (model 1a)	Later	Southward	Large	30 Ma
Reference Double-sided (model 1b)	Later	Double-Sided	Large	30 Ma
Refined Southward (model 2a)	Early	Southward	Small	45 Ma
Refined Double-sided (model 2b)	Early	Double-Sided	Small	45 Ma

3. Results

3.1 Reference Southward Subduction (Model 1a)

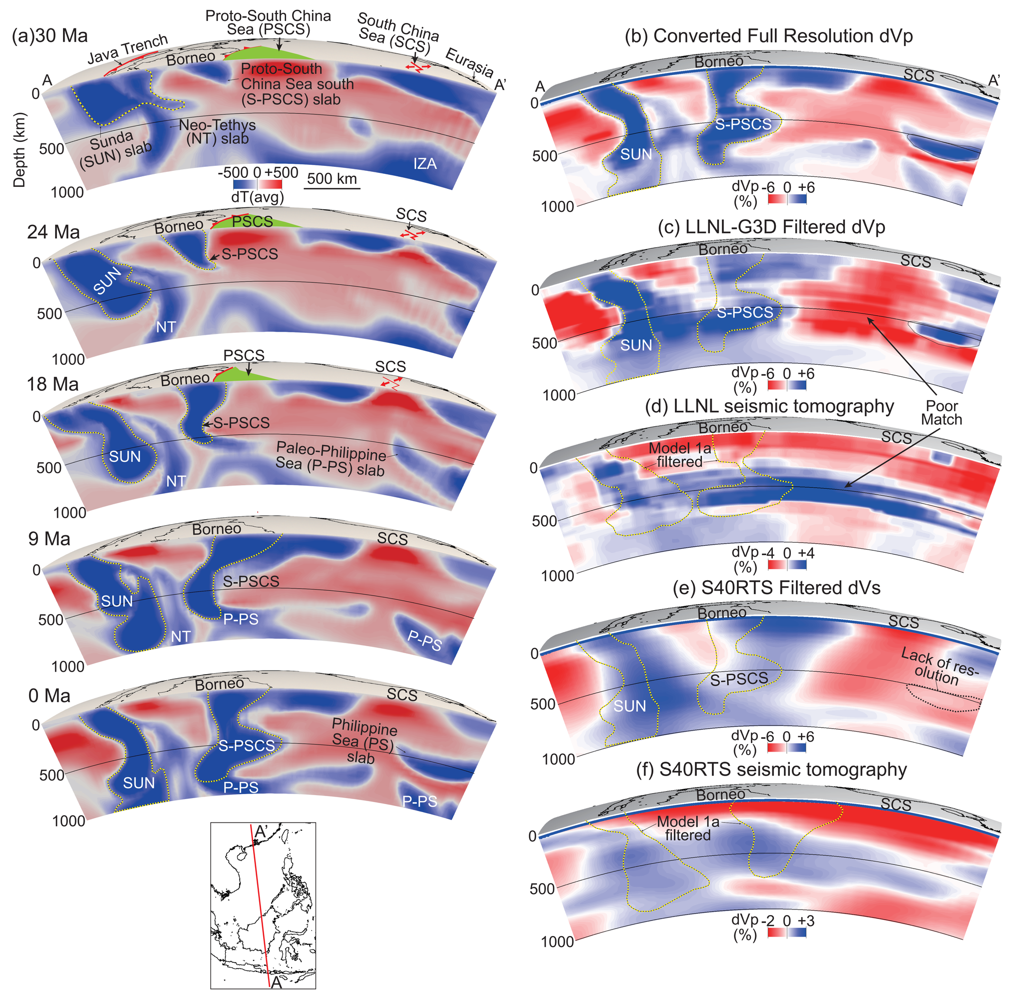

• Results of the reference Model 1a that implemented southward PSCS subduction. (a) 3D visualizations of the time-dependent mantle thermal structure evolution for the reference southward subduction model 1a from 30 to 0 Ma. The top surface shows the PSCS in green and reconstructed Borneo coastlines. At 0 Ma (present-day), the southward-subducted proto-South China Sea (S-PSCS) slabs are located at ~400-800 km depths beneath Borneo. (b) The 0 Ma temperature field from a) converted to a full-resolution P-wave perturbation (dVp) following Schuberth et al. (2009).
• (c) Cross-section in (b) filtered through the LLNL-G3D resolution operator (Simmons et al., 2019) to show a 'synthetic tomography' of the 0 Ma geodynamic model. (d) Comparison to section co-located to (c) from actual LLNL-G3D-JPS P-wave seismic tomography model (Simmons et al., 2016). The Sunda (SUN) slabs are generally reproduced but a mismatch exists under the present SCS.
• (e) S40RTS resolution operator (Ritsema et al., 2011) was applied to (b). The cold slabs under the northern SCS in (b) are not seen in (e), indicating lack of resolution in these areas. (f) Comparison of (e) to actual S40RTS S-wave seismic tomography model (Ritsema et al., 2011).
• The comparison between predicted and imaged mantle structure from S-waves shows the Sunda slabs are generally reproduced but a mismatch exists under the SCS, similar to the P-wave comparison in (c) and (d).

3.2 Reference Double-Sided Subduction (Model 1b)

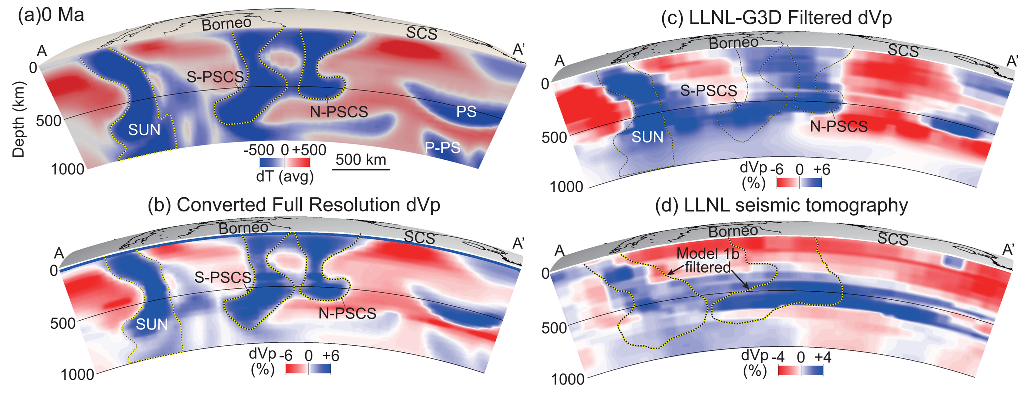

• Results of the reference Model 1b that implemented a similar input plate model to Model 1a but invoked double-sided PSCS subduction. (a) At 0 Ma, the predicted present-day S-PSCS is at ~400-800 km depths beneath Borneo and the northward-subducted PSCS slabs (N-PSCS) is at ~400-500 km depths beneath the southern SCS. (b) The temperature field from a) at 0 Ma converted to dVp following Schuberth et al. (2009). (c) Cross-section in (b) filtered through the LLNL-G3D resolution operator (Simmons et al., 2019).
• (d) Comparison of (c) to actual LLNL-G3D-JPS P-wave seismic tomography model (Simmons et al., 2016) across the same location. The SUN slabs are generally reproduced in the geodynamic model but the sub-horizontal slabs under the SCS do not match well to the geodynamic model.

3.3 Refined Model (Model 2a and 2b)

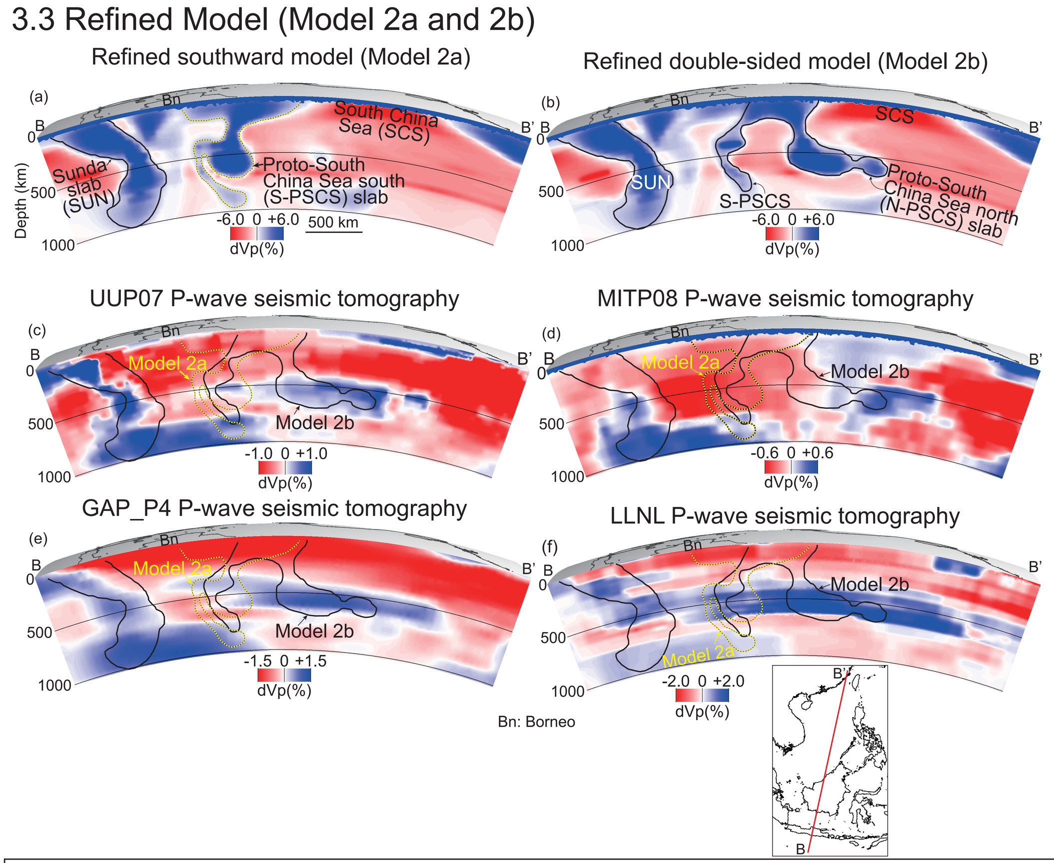

• (a) 0 Ma mantle structure predicted from the refined southward subduction model 2a shows the southward-subducted S-PSCS slabs at ~400-1000 km depths under Borneo. (b) The refined double-sided model 2b shows S-PSCS slabs at ~400-1000 km depth under Borneo and northward-subducted N-PSCS slabs at ~500-700 km depths under the southern SCS.

• Comparison between global P-wave seismic tomography models (c-f) and the geodynamic models (yellow and black outlines) across B-B' shows that the N-PSCS slabs in Model 2b has a better match to the sub-horizontal slabs under the present SCS in tomography at 400 to 700 km depths. Thus we conclude that Model 2b is our preferred model.

4. Discussion

4.1 Comparison to Tomographic Vote Map
(GAP04, MITP08, UUP07)

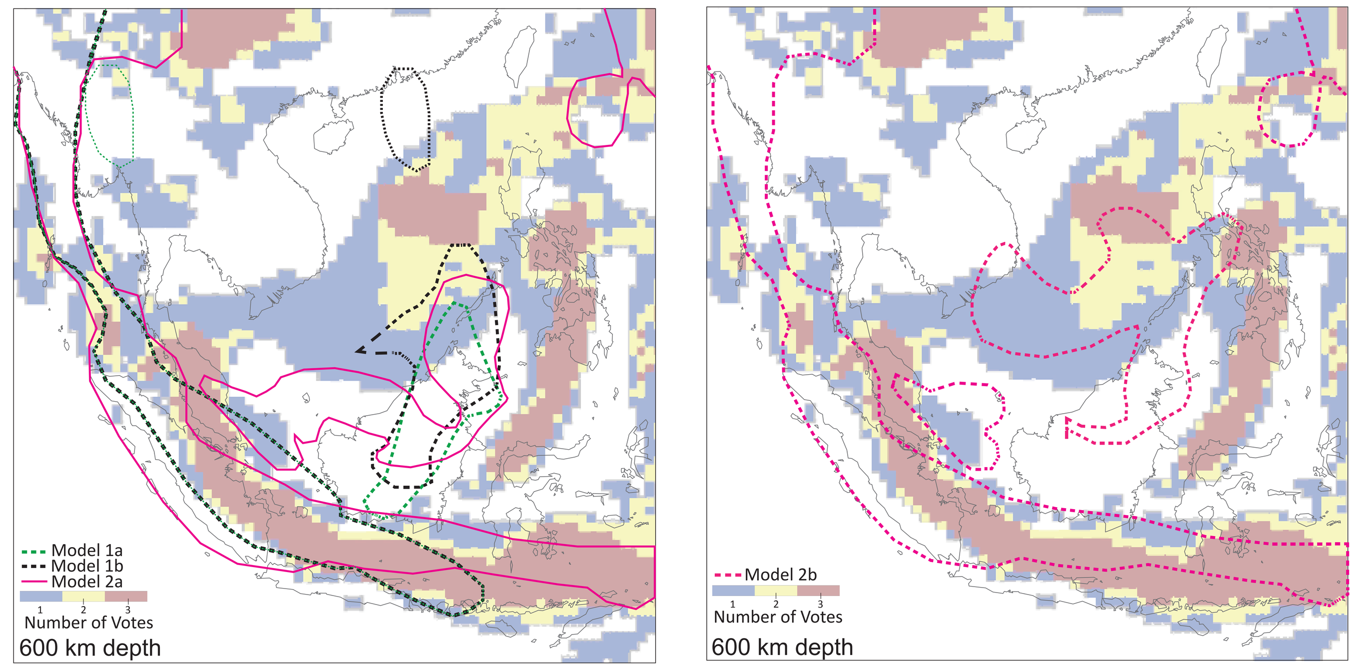

• Fast-anomaly vote maps from MITP08, GAP_P4 and UUP07 seismic tomography model at 600 km depths in comparison to models 1a, 1b, 2a, and model 2b. Color lines indicate the fast anomalies from the full resolution, dVp- converted geodynamic model results. All models generally reproduce the Sunda slabs. **Model 2b was able to better reproduce the slabs under the present SCS and therefore, is our preferred model.**

4.2 Correlation between Geodynamic Model and Tomography

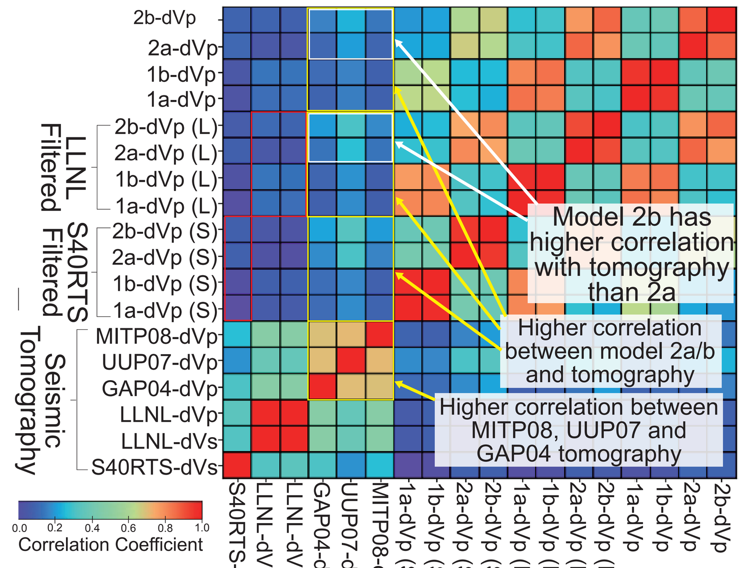

• Color-coded correlation coefficient matrix showing similarities between various geodynamic models, seismic tomography models, and geodynamic models v.s. seismic tomography models at 400-600 km depths. Models 2a and 2b show higher correlations to seismic tomography models relative to Models 1a and 1b.
• The global P-wave seismic tomography models MITP08 (Li et al., 2008),GAP_P4 (Fukao & Obayashi, 2013) and UUP07 (Amaru, 2007) show ~0.6-0.8 correlations relative to each other. The correlation between geodynamic models and seismic tomography models is ~0.2 correlation, which is comparable to global averages for degree 1-20 (Shephard et al., 2012)

4.3 Where are the proto-South China Sea slab ?

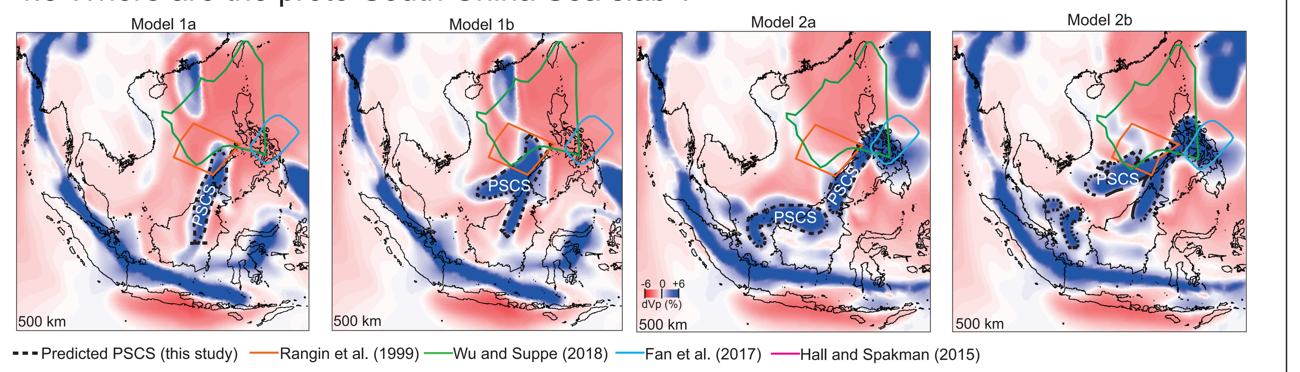

• When all four models are considered together, ourgeodynamic models generally predict the PSCS slabs are under eastern Borneo, the present SCS, the Sulu Seamthe Celebes Sea, and the southern Philippines between 500 to 800 km depths (black dashed lines).
• Slabs under the central Philippines is predicted from various sources: subducting a vanished ocean, a large Philippines Sea plate, or the PSCS; therefore, some caution is needed when inferring the plate tectonic histories of slabs under the central Philippines.

4.4 Predicted Mantle Flow from preferred Model 2b

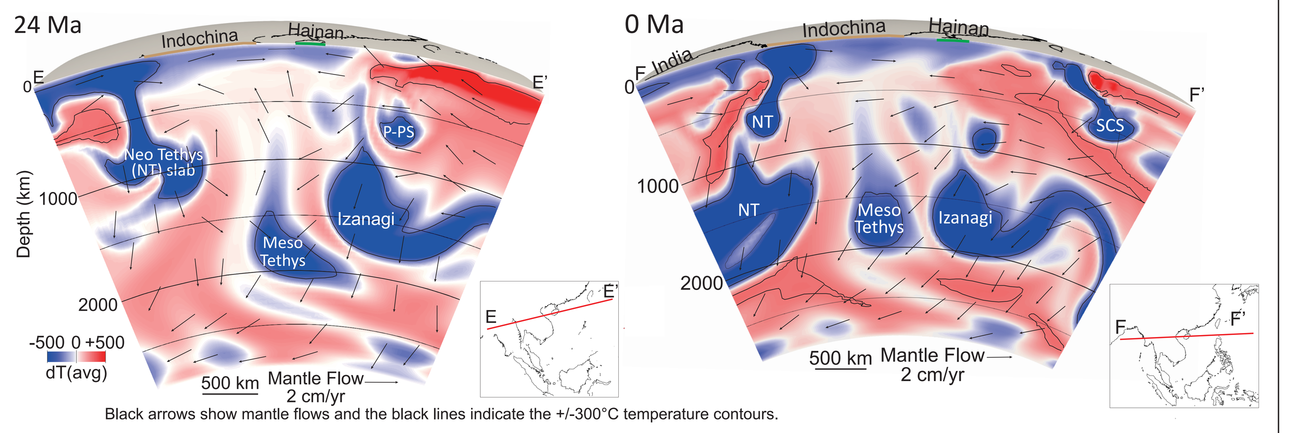

Black arrows show mantle flows and the black lines indicate the +/-300°C temperature contours.

• Predicted mantle flows and mantle structures from model 2b under Indochina and Hainan Island predict a mid-mantle convective upwelling beneath Indochina and Hainan.
• All four models produced similar mantle flows in this region. This shows the predicted mantle flow of the preferred model (model 2b).
• Extensive downwelling beneath SCS at 0 Ma does not support the idea of deep-origin 'Hainan' mantle plume.

4.5 Predicted Dynamic Topography

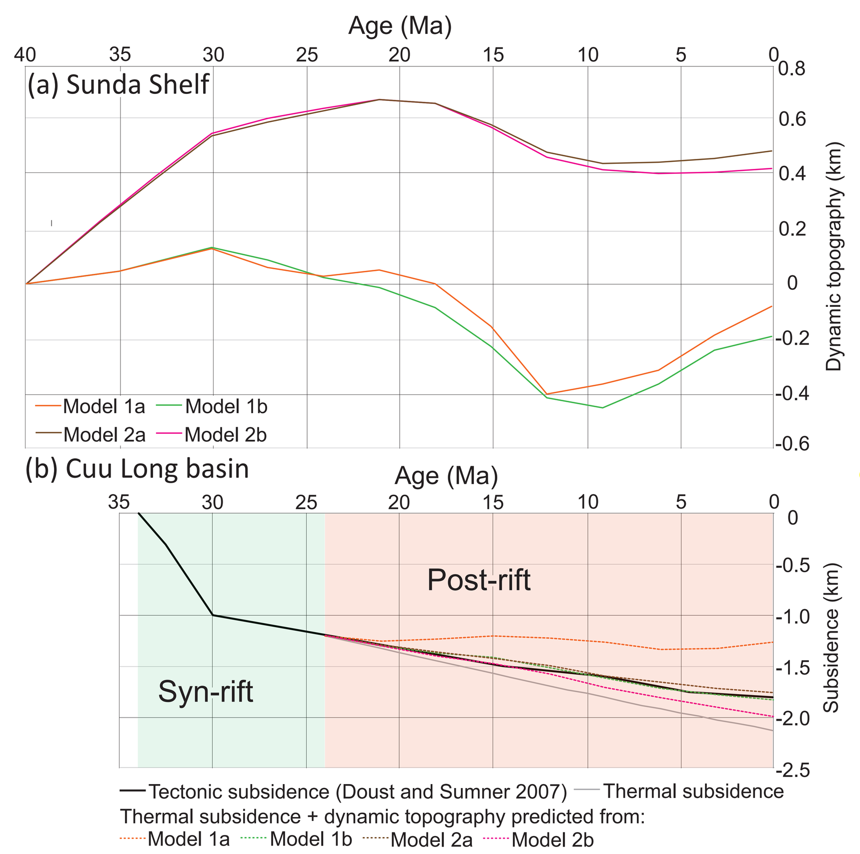

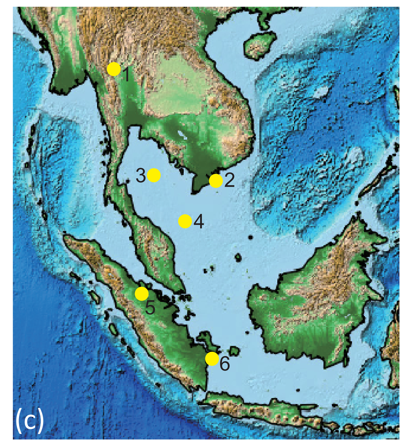

• Basins used to calculated average Sunda shelf dynamic topography; 1: Phitsanulok, 2: Quay Long, 3:Pattani, 4: Malay, 5: Central Sumatra, 6: Sunda

• Dynamic topography predicted by the geodynamic models in this study. (a) Models 1a, 1b, 2a and 2b shows highly contrasted dynamic topography histories at Sunda shelf. This suggests that dynamic topography predictions are strongly dependent on the input plate model, which are controversial. (b) Comparison between observed and predicted tectonic subsidence at the Cuu Long basin, offshore Vietnam. (c) Map showing the sedimentary basins used to calculate an average Sunda shelf dynamic topography.
• At the post-rift stage there is ~400 m vertical discrepancy between the observed tectonic subsidence (black line) and the modeled thermal subsidence (grey line). By adding the predicted dynamic topography to thermal subsidence, we show a better fit the predicted total tectonic subsidence (colored dashed lines). Models 1b and 2a yield the best match to the observed subsidence.

Reference
Advokaat, E.L., Marshall, N.T., Li, S., Spakman, W., Krijgsman, W., van Hinsbergen, D.J.J., 2018. Cenozoic Rotation History of Borneo and Sundaland, SE Asia Revealed by Paleomagnetism, Seismic Tomography, and Kinematic Reconstruction. Tectonics 37, 2486-2512.
Amaru, M.L., 2007. Global travel time tomography with 3-D reference models: Geologica Ultraiectina, (PhD Thesis), p. 174.
Boyden, J.A., Müller, R.D., Gurnis, M., Torsvik, T.H., Clark, J.A., Turner, M., Ivey-Law, H., Watson, R.J., Cannon, J.S., 2011. Next-generation plate-tectonic reconstructions using GPlates, in: Baru, C., Keller, G.R. (Eds.), Geoinformatics: Cyberinfrastructure for the Solid Earth Sciences. Cambridge University Press, Cambridge, pp. 95-114.
Cullen, A.B., 2010. Transverse segmentation of the Baram-Balabac Basin, NW Borneo: refining the model of Borneo's tectonic evolution. Petroleum Geoscience 16, 3-29.
Doust, H., & Sumner, H. S. (2007). Petroleum systems in rift basins a collective approach in Southeast Asian basins. Petroleum Geoscience, 13(2), 127 144.
Fan, J., Zhao, D., Dong, D., Zhang, G., 2017. P-wave tomography of subduction zones around the central Philippines and its geodynamic implications. Journal of Asian Earth Sciences 146, 76-89.
Fukao, Y., Obayashi, M., 2013. Subducted slabs stagnant above, penetrating through, and trapped below the 660 km discontinuity. Journal of Geophysical Research: Solid Earth 118, 5920-5938.
Fuller, M., Ali, J.R., Moss, S.J., Frost, G.M., Richter, B., Mahfi, A., 1999. Paleomagnetism of Borneo. Journal of Asian Earth Sciences 17, 3-24.
Hall, R., 2012. Late Jurassic–Cenozoic reconstructions of the Indonesian region and the Indian Ocean. Tectonophysics 570-571, 1-41.
Hall, R., Spakman, W., 2015. Mantle structure and tectonic history of SE Asia. Tectonophysics 658, 14-45.
Li, C., van der Hilst, R.D., Engdahl, E.R., Burdick, S., 2008. A new global model for P wave speed variations in Earth's mantle. Geochemistry, Geophysics, Geosystems 9, Q0501.
Matthews, K.J., Maloney, K.T., Zahirovic, S., Williams, S.E., Seton, M., Müller, R.D., 2016. Global plate boundary evolution and kinematics since the late Paleozoic. Global and Planetary Change 146, 226-250.
Rangin, C., Spakman, W., Pubellier, M., Bijwaard, H., 1999. Tomographic and geological constraints on subduction along the eastern Sundaland continental margin (South-East Asia). Bulletin de la Société Géologique de France 170, 775-788.
Ritsema, J., Deuss, A., van Heijst, H.J., Woodhouse, J.H., 2011. S40RTS: a degree-40 shear-velocity model for the mantle from new Rayleigh wave dispersion, teleseismic traveltime and normal-mode splitting function measurements. Geophysical Journal International 184, 1223-1236.
Schuberth, B. S. A., Bunge, H. P., Steinle Neumann, G., Moder, C., & Oeser, J. (2009). Thermal versus elastic heterogeneity in high resolution mantle circulation models with pyrolite composition: High plume excess temperatures in the lowermost mantle. Geochemistry, Geophysics, Geosystems, 10(1).
Simmons, N. A., Myers, S. C., Johannesson, G., Matzel, E., & Grand, S. P. (2015). Evidence for long lived subduction of an ancient tectonic plate beneath the southern Indian Ocean. Geophysical Research Letters, 42(21).
Simmons, N. A., Schuberth, B. S. A., Myers, S. C., & Knapp, D. R. (2019). Resolution and Covariance of the LLNL G3D JPS Global Seismic Tomography Model: Applications to Travel time Uncertainty and Tomographic Filtering of Geodynamic Models. Geophysical Journal International, 217(3), 1543-1557.
Wu, J., Suppe, J., 2018. Proto-South China Sea Plate Tectonics Using Subducted Slab Constraints from Tomography. Journal of Earth Science 29, 1304-1318.
Wu, J., Suppe, J., Lu, R., Kanda, R., 2016. Philippine Sea and East Asian plate tectonics since 52 Ma constrained by new subducted slab reconstruction methods. Journal of Geophysical Research: Solid Earth 121, 4670-4741.